

Harnessing Thor's Hammer: Experimentally induced lightning trauma to human bone by high impulse current

Nicholas Bacci^a, Tanya Nadine Augustine^{a,*}, Hugh G.P. Hunt^b, Ken J. Nixon^b,
Jakobus Hoffman^c, Lunga Bam^c, Frikkie de Beer^c, Patrick Randolph-Quinney^{d,e,**}

^a School of Anatomical Sciences, Faculty of Health Sciences, University of the Witwatersrand Medical School, Johannesburg, South Africa

^b The Johannesburg Lightning Research Laboratory, School of Electrical and Information Engineering, Faculty of Engineering and the Built Environment, University of the Witwatersrand, Johannesburg, South Africa

^c Department Radiation Utilisation, South African Nuclear Energy Corporation SOC Ltd. (Necsa), Pelindaba, South Africa

^d Forensic Science Research Group, School of Applied Sciences, Faculty of Health and Life Sciences, Northumbria University, Newcastle Upon Tyne, Northumbria, NE1 8ST, UK

^e Centre for the Exploration of the Deep Human Journey, University of the Witwatersrand, Johannesburg, South Africa

ARTICLE INFO

Keywords:

Lightning
Bone trauma
Forensic taphonomy
High current impulse
Micro-focus X-ray computed tomography
Histology

ABSTRACT

Lightning fatality identification relies primarily on soft tissue traumatic pattern recognition, prohibiting cause of death identification in cases of full skeletonisation. This study explores the effects of high impulse currents on human bone, simulating lightning-level intensities and characterising electrically induced micro-trauma through conventional thin-section histology and micro-focus X-ray computed tomography (μ XCT). An experimental system for high impulse current application was applied to bone extracted from donated cadaveric lower limbs ($n = 22$). μ XCT was undertaken prior to and after current application. Histological sections were subsequently undertaken. μ XCT poorly resolved micro-trauma compared to conventional histology which allowed for identification and classification of lightning-specific patterns of micro-trauma. Statistical analyses demonstrated correlation between current intensity, extent and damage typology suggesting a multifaceted mechanism of trauma propagation - a combination of electrically, thermally and pressure induced alterations. This study gives an overview of high impulse current trauma to human bone, providing expanded definitions of associated micro-trauma.

1. Introduction

Lightning is a common and often hazardous natural phenomenon. Real storm observation-based approximations suggest a worldwide lightning flash density of 6 flashes/km²/year [1]. However, higher lightning flash densities are seen in certain countries, such as South Africa with a rate between 10 and 15 lightning flashes/km²/year in some areas, likely due to the high altitude in the escarpment regions [2].

Lightning can result in substantial financial losses in damage to business and homeowners as well as loss of life. Recent estimates for the United States of America reported \$790 million in damages being claimed from homeowners' insurance for lightning-based damage in

2015 alone [3]. In addition, lightning is implicated in the death of livestock, zoological garden and game park animals, resulting in substantial financial costs [4]. Recorded lightning animal fatalities have included from as few as one, to as many as 850 animals in a single incident [4].

Global lightning fatality rates are elusive due to sporadic reporting and underreported figures from different countries [3,5]. The most recently available estimates, originating from 28 countries, suggest that between 4429 and 24,000 lightning fatalities occur annually worldwide [6]. The least affected countries appeared to be found in Europe, with annual fatality rates ranging between 0.1 and 0.4 deaths per million [3, 6]. North America had similarly low fatality rates with the exclusion of

* Corresponding author. 7 York Road, Parktown, 2193, School of Anatomical Sciences, Faculty of Health Sciences, University of the Witwatersrand, Johannesburg, South Africa.

** Corresponding author. Forensic Science Research Group, Department of Applied Sciences, Faculty of Health and Life Sciences, Northumbria University, Newcastle upon Tyne, Northumbria, NE1 8ST, United Kingdom.

E-mail addresses: tanya.augustine@wits.ac.za (T.N. Augustine), patrick.randolph-quinney@northumbria.ac.uk (P. Randolph-Quinney).

<https://doi.org/10.1016/j.fsisy.2021.100206>

Received 25 July 2021; Received in revised form 14 October 2021; Accepted 14 October 2021

Available online 3 November 2021

2589-871X/© 2021 The Authors.

Published by Elsevier B.V. This is an open access article under the CC BY-NC-ND license

(<http://creativecommons.org/licenses/by-nc-nd/4.0/>).

Table 1
Details of cadaveric sample pool.

Age	Sex	Ancestry	Weight (kg)	Height (m)	Cause of Death
≈60	Male	European	58	1.84	Natural causes
56	Male	European	81	1.87	Myocardial infraction
60	Female	European	41	1.67	Natural causes
92	Female	European	73	1.61	Unknown

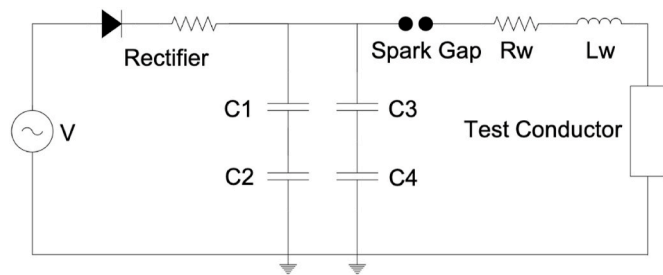


Fig. 1. Schematic of an 8/20µs impulse generator utilized to simulate lightning currents. The capacitor bank (C1, C2, C3, C4) are charged, when the spark gap fires, the charge then flows through R_w and L_w which shape the rise and fall-time. This high-current impulse is then delivered to the Test Conductor or Object as if it were ‘struck by lightning’.

Mexico (2.7 deaths/million/year) [3,6]. In Asia, China and Japan reported relatively low fatality rates, while other countries indicated intermediate fatality rates similar to Mexico and South American countries [3,6]. African countries, however, appear to have some of the highest fatality rates, with South Africa, Swaziland and Malawi reporting as many as 6.3, 15.5 and 84.0 deaths/million/year respectively [3,6]. This is due to several factors, including lack of ‘lightning safe’ infrastructure, high flash densities and poor safety awareness [3,7].

Lightning fatalities are often not as evident as fatalities from other large-scale weather events such as heatwaves, hurricanes, and flooding. This scattered and isolated nature of individual lightning-related fatalities can severely hinder their identification when human remains are recovered [3].

Determining the occurrence of a lightning fatality is traditionally dependent on soft tissue analysis and circumstantial evidence [7,8]. Published case studies [9,10] propose that lightning strike and high impulse currents cause ventricular fibrillation, cardiac arrest, respiratory arrest and asphyxia [11,12]. Forms of injury documented in lightning fatalities include neurological trauma [13], rupture of the tympanic membranes [12,14], cutaneous ferning patterns (Lichtenberg figures) [15], unilateral or bilateral clavicular fractures [16], shrapnel trauma [14], and specific types of electrical burns, particularly on the soles of the feet [14,17]. While occasionally severe burns along the current’s entry and exit sites have been observed [18], the absence of electrical burns can further complicate manner of death identification [12]. Understanding the current’s distribution through the body can aid in interpreting injuries and traumatic events. Computer-simulated multi-tissue models of high impulsive current events found that 11% of the total current density experienced by the sample was distributed within the vascular network, with 85% of it being distributed through muscle, 3.5% through fat and only 0.5% through cortical bone and bone marrow [19].

These pathophysiological effects have historically been noted to affect the soft rather than hard tissues, and until recently, the effect of lightning energy on the skeletal system was unknown. In a recent proof of concept animal study we detailed specific traumatic effects related to high impulse current application [20] to a pig bone sample, and contrasted this with a case of lightning-fatality on a wild giraffe. Microscopically, extensive micro-fracturing and fragmentation of the bone matrix was observed, which we interpreted as being associated with current flow through and between osteon units; this indicated that lightning trauma is not solely limited to the soft tissues [20]. In our non-human study we suggested that micro-fracturing was broadly comparable to patterned micro-fracturing observed in burnt bone, but

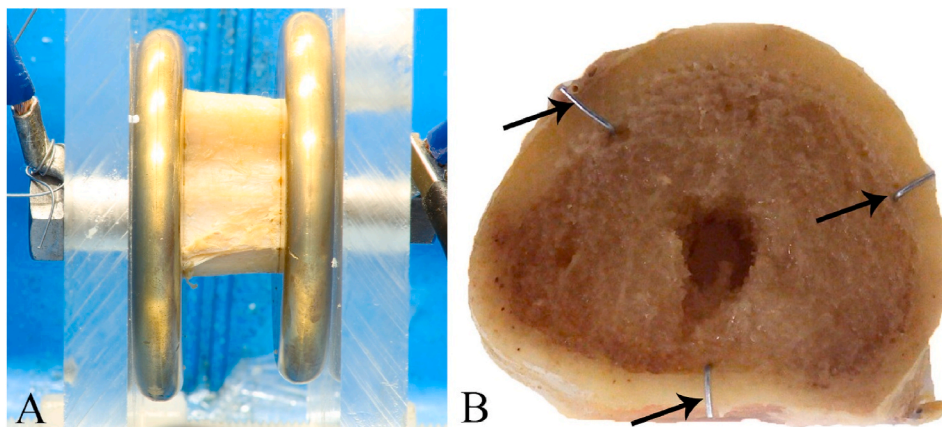


Fig. 2. Modes of current application to bone samples. Image A demonstrates the parallel plate current application (PPA) standardized testing procedure. Image B demonstrates the wire arrangement (black arrows) in the wire-directed impulse application (WDA) testing procedure.

Table 2
Outline of resulting peak residual voltages and peak currents for each charging potential.

Charging Potential (kV)	Minimum Vp (kV)	Maximum Vp (kV)	Mean pV (kV)	Minimum Ip (kA)	Maximum Ip (kA)	Mean Ip (kA)
3.5	3.28	3.84	3.65	0	0	0
4	4.24	4.28	4.26	1.12	1.28	1.20
6	6.24	6.56	6.43	6.72	8.72	8.01
6.5	1.12	7.04	4.97	9.28	9.44	9.36

Each charging potential is tabulated here with their respective minimum, maximum, and mean peak residual voltage (Vp) and peak current (Ip). Note that for increased charging voltages, higher peak currents are generated.

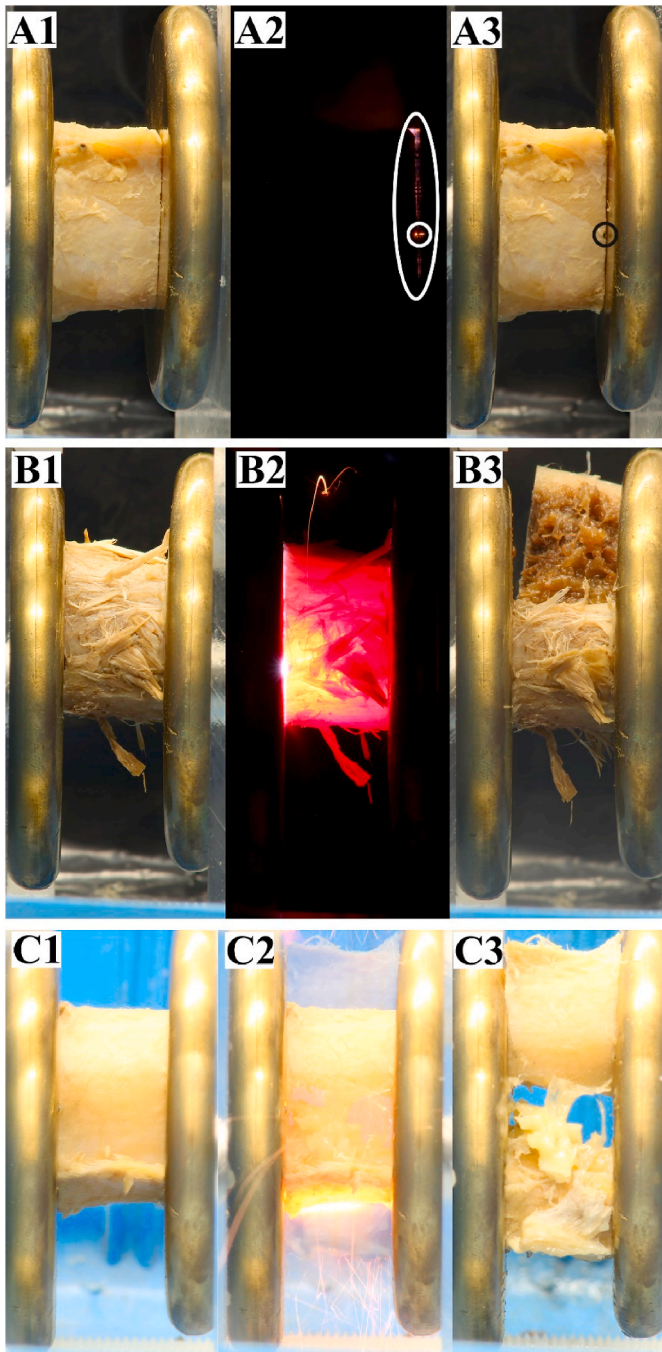


Fig. 3. Plate including three sets of long exposure photographs of observed flashing before (left), during (middle), and after (right) wire-directed impulse application. Series A highlights the current traversing the bone block through small discharges between it and the brass plate (white ellipse) with a particularly brighter flash (white circle), which resulted in singeing bone and surrounding soft tissues. Series B demonstrates the passage of the current within the bone or bone marrow cavity, resulting in a splitting of the bone section. Series C shows the extreme instantaneous fragmentation of the bone block as a result of the impulse application.

with several important areas of difference - thermally induced micro-fractures are but a limited part of the much broader system of patterned thermal destruction of the human body [21]. Thermal alteration of the human body is a complex one caused by the disparate physical and biochemical structures of the human body [22]. All the systems of the body are capable of thermal destruction, including the hard tissues. Many systems actively contribute to the burning process of

intrinsic fuels sources; subcutaneous body fat, organ fat, volatile organic components, and bone marrow all contribute to the overall fuel load. However, the combustion of the hard tissues is fundamentally different from other organ systems due to the multiphase nature of bone. Bone is composed of physiologically bound organic materials that exhibit both a crystalline and amorphous phase (primarily type I collagen, with glycosaminoglycans [GAGs] and other protein constituents), as well as an inorganic matrix of hydroxyl or bioapatite (inorganic salts largely made up of calcium and phosphorus), which again exhibits both a crystalline and amorphous phase, and water [21–23]. As such, bone burns in a very different manner from other tissues, due to the high proportion of inorganic matrix [23].

The general pattern of thermal change and destruction of bone is well-understood [21,23]. At its most basic level the burning of bone represents the processes of dehydration and recrystallisation as a direct function of both increasing temperature and length of burning [21,23,24]. Specifically, this leads to the initial removal of physiosorbed and chemisorbed water from bone [22,23,25]. This is followed by thermal decomposition of organic components such as collagen and GAGs, which leads to the conversion (inversion) of hydroxyapatite to β -tricalcium phosphate, and eventually the fusion and recrystallisation of the remaining inorganic part [22,23,25]. This four-stage process leads to a series of recognisable gross morphological, macrostructural and microstructural changes [22,23] which are quantifiably and qualitatively different from the traumatic patterns seen in lightning alteration in animal bone. However, no clear understanding of the changes seen because of lightning (a high impulse current, reaching kiloampere's but only for microseconds) on bone exists beyond the work of Bacci and colleagues [20], with no studies until today being conducted on human bone. Due to ultrastructural differences between human and non-human bone [26] this study aimed to investigate whether high impulse currents caused lightning-specific patterns of trauma in human skeletal tissue.

2. Materials and preparation

All samples used in this study comprise femora and tibiae of embalmed cadavers (Table 1), from the Cadaveric Collection of School of Anatomical Sciences, Faculty of Health Sciences, University of the Witwatersrand, Johannesburg. Ethics clearance was granted by the Human Research Ethics Committee (Medical) (Human Ethics Waiver No.: W-CJ-14064-1).

2.1. Demographics of each cadaver sampled and cause of death

Selected samples showed no external signs of ante-mortem trauma or surgical intervention. Following sample selection, femora and tibiae were macerated by manual dissection. Two 2 cm diameter cylindrical blocks were extracted from each femur and tibia using an EXAKT 312 Pathology Saw. Sectioning sites were located: 1) 12 cm from the most proximal aspect of the femur and 10 cm from the most distal aspect of the femur; 2) 8 cm from the most proximal aspect of the tibia and 6 cm from the most distal aspect of the tibia. A total of 25 bone blocks were extracted, three of which were selected as control specimens, leaving a total of 22 blocks that were used in the experimental procedure.

The experimental procedure utilized a high-voltage impulse generator with the capacity to generate an 8/20 μ s impulse current of up to approximately 15 kA (Fig. 1). The 8/20 μ s impulse generator delivered a current with an 8 μ s rise, defined as the time necessary for accumulation of the peak charge, and a 20 μ s fall time [27]. Experimentation was conducted at the following charging potentials, 3.5, 4, 6, and 6.5 kV. Charging potential (CP) was defined as the approximate potential difference charged over the capacitor bank of the impulse generator prior to current application. It is commonly referred to as charging voltage in the context of impulse current testing – the higher the charging potential, the higher the peak of the generated impulse current [28]. These testing CPs were selected to preserve sample viability, since during

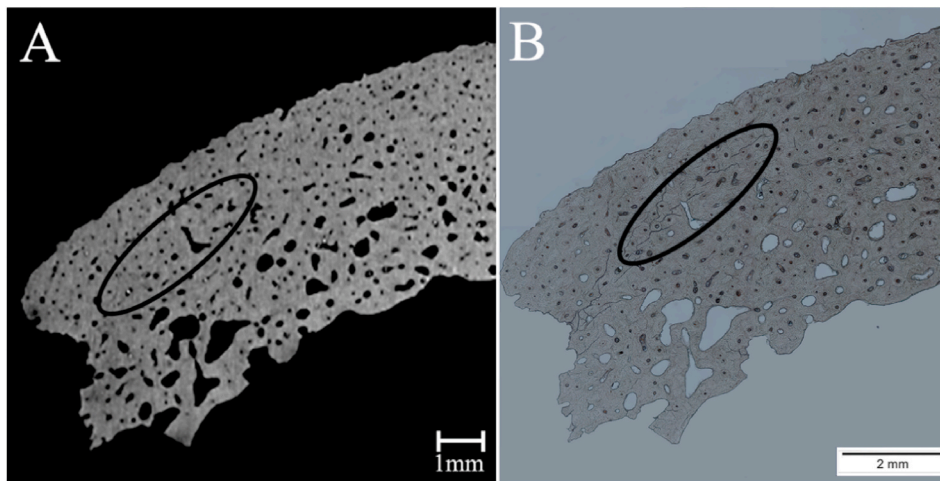


Fig. 4. Visual comparison of microfocus CT transverse orthoslice (A) and histology photomicrograph (B). Orthoslice (A) of the same sample shows no microfracturing, due to limited resolution. Photomicrograph (B) shows a large micro-fracture at low magnification ($\times 10$).

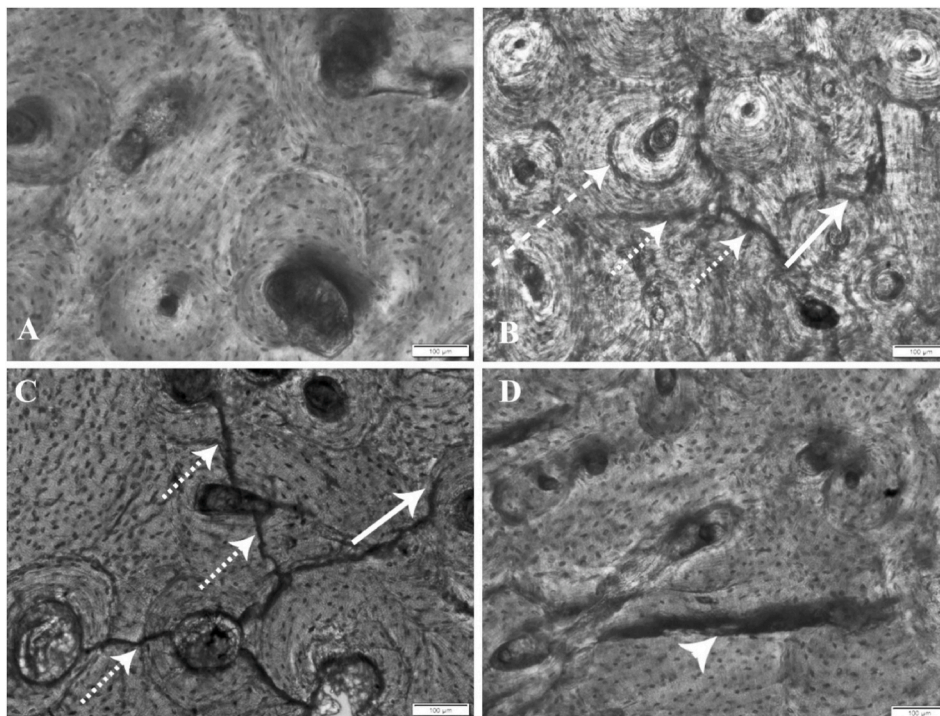


Fig. 5. Photomicrographs of human bone showing a control section (A) contrasted with different types of micro-fractures (B–D) identified in experimental samples. Note the radiating (dotted arrows), circumferential (dashed arrow), circumferential irregular (full arrows) and irregular (arrowhead) micro-fracture types as seen in specimens from this study.

optimisation higher charging potentials resulted in extensive damage to the bone. Measurements of the peak voltage (V_p) and peak current (I_p) intensities, as well as its passage through the test specimens, were recorded with a GRS-6052A oscilloscope (GW Instek). Peak voltage was defined as the peak of the residual voltage over the testing area following the electrical system completion during each discharge of the current, and it relates directly to the residual electric field over the testing area [29]. Peak current was defined as the peak effective current that flowed through the testing material, usually as breakdown of the insulating nature of the material occurred [29].

Optimisation was conducted on eight randomly selected blocks ($n = 8$). Different CP thresholds of 1 kV ($n = 1$), 2 kV ($n = 2$), 5 kV ($n = 1$), 8 kV ($n = 2$), and 10 kV ($n = 2$) were applied in the optimisation process.

Two distinct modes of current impulse application were employed, parallel plate impulse application (PPA) and wire-directed impulse application (WDA). With PPA, blocks were placed between two flat brass plates with the proximal aspect of the bone block directed at the current's entry point (Fig. 2A). WDA involved inserting three steel wire segments equidistantly on the bone block directly below cortical bone, within the trabecular bone matrix of the blocks, prior to placement between the parallel plates (Fig. 2B).

All impulse application procedures were recorded with 8 s long-exposure photography (Canon EOS 7D, EFS 18–55 mm lens), to visualise current conduction and passage. Samples were also photographed prior to and following experimental impulse application to identify signs of macroscopic damage.

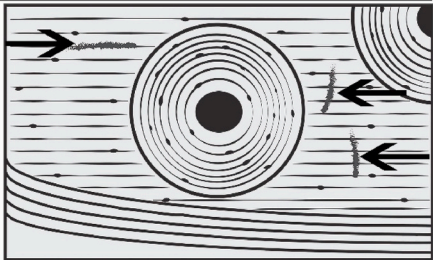
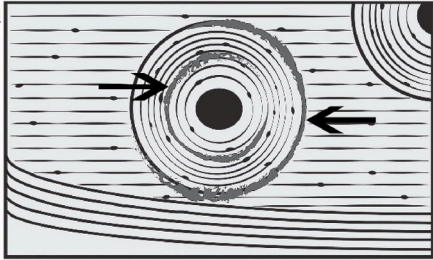
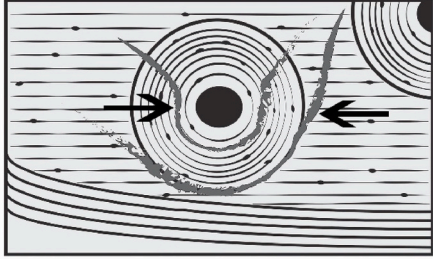
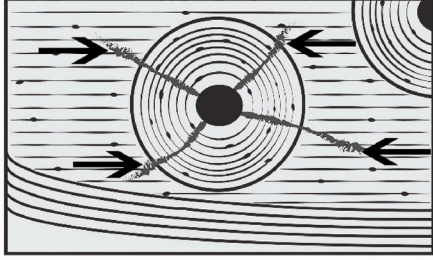
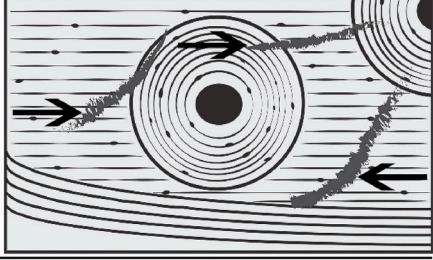
Micro-fracture classification	Descriptive criteria	Visual depiction
Interstitial	Short, thin, linear micro-fractures found in parallel or relatively perpendicular to interstitial lamellae.	
Circumferential	Short, curvilinear micro-fractures located within the concentric lamellae of an osteon or along the cement line of an osteon, following a circular trajectory. May appear to cause delamination from the surrounding interstitial lamellae.	
Circumferential irregular	Elongated curvilinear micro-fractures within the concentric lamellae of an osteon, extending beyond the boundaries of the cement line and into the surrounding interstitial lamellae. Extensions are linear and parallel to the interstitial lamellae. Occasionally seen to merge with other micro-fracture types.	
Radiating	Linear straight or undulating micro-fractures extending from the osteonic canal, perpendicular to the concentric lamellae, and up to or beyond the cement line in an outwards radiating pattern. They start wide proximally to the osteonic canal and narrower as they extend distally. Commonly found in multiples and may merge with other micro-fractures.	
Irregular	Micro-fractures that extend beyond the scope of the above definitions, commonly used when multiple fracture networks merge. These micro-fractures tend to be particularly extensive and wider than most other classifications, crossing multiple histological areas and with inconsistent shape or course.	

Fig. 6. Cortical bone micro-fracture classification definition with associated visual representation (observationally adapted from Brain, 1993 [35]). Classifications are defined based on regional and histomorphological appearance of micro-trauma observed and depicted in diagrams as dark grey fractures (arrows).

Following experimentation all bone blocks, including controls, were processed for analysis. Two thin-sections were obtained from each of the 25 blocks (section n = 50) via sectioning with a high-speed Clarke® CRT40 - 40pce rotary tool equipped with DREMEL® cut-off wheel No. 409. Thereafter any adherent overlying soft tissue was mechanically removed, and the sections submerged in distilled water. Sections were manually ground to thin sections on 220 grit waterproof carborundum paper lubricated with 10–20 ml distilled water as per Maat and colleagues [30] ground bone thin-section method. During this process, sections were assessed using light microscopy for the presence of identifiable histological features. Once this was achieved, sections were rinsed three times in distilled water and placed in a fresh change of

distilled water to prevent dehydration prior to mounting.

Sections were mounted, cover-slipped with Entellan®, and viewed unstained using light microscopy to establish the extent and typology of electrically induced damage to tissue. Photomicrographs were taken of observed alterations to the bone tissue using an Olympus iX51 Inverted Microscope with CellSens software (v. 10).

3. Analytical methods

Quantitative analysis of micro-fractures was performed on three photomicrographs from each section with representative cohorts of charging potentials from both PPA and WDA specimens. A

Table 3
Comparative summary of electrical and thermal microstructure alterations.

Gross and Histological alterations	Lightning trauma	Thermally altered bone	References
Irregular longitudinal fractures	No	Yes	[22,35]
Transverse curvilinear fractures	No	Yes	[22,35]
Soot and organic material deposition	No	Yes	[22,35]
Colour changes	No	Yes	[23,24,35]
Shape distortion and dimensional change	No	Yes	[22,24,35]
Surface patination	No	Yes	[22,35]
Thumbnail fractures	No	Yes	[22,35]
Radiating micro-fracturing	Yes	Yes	[20,43]
Circumferential micro-fracturing	Yes	Yes	[35,43]
Circumferential irregular micro-fracturing	Yes	Yes	[35,43]
Irregular micro-fracturing	Yes	Yes	[35,44,45]

Summary of the observed bone histological alterations is presented comparing occurrences observed in the high impulse current experiments and similarities described in burnt bone literature as characteristic of heat-induced skeletal modifications.

representative sample of 14 blocks, including the three control blocks, were selected for quantitative analysis. The charging potentials at which these selected blocks were experimented upon, included 3.5, 4, 6, and 6.5 kV since during optimisation intensities greater than 6.5 kV with WDA application caused fragmentation of samples.

3.1. Photomicrography

Images were acquired and measured using CellSense software (Olympus iX51, v. 10). Section length was measured and then subdivided into ten equal intervals. Representative photomicrographs were obtained in the field of view at the first, fifth and ninth interval. For each field of view, the fracture number (FN) was recorded and the following measurements taken:

- Fracture Area (FA): obtained by demarcating the outer borders of the fractures manually through the software's closed polygon measuring tool
- Fracture Length (FL): measured using a polyline measuring tool, along the midline of the entire extent of individual fractures
- Fracture Perimeter (FP): calculated by CellSens from the manually demarcated fracture area outline.
- Total fractured area (TFA) was also calculated for each field of view and a ratio (TFA/TBA) was created by contrasting to the total bone area (TBA) defined as total observable bone area in a field of view.

Intra- and inter-observer error were calculated through intra-class correlation tests (SPSS v.20). Chi-squared tests were conducted to identify differences between fracture types and current application mode, with post-hoc analysis through computation of adjusted residuals (z-scores) and Bonferroni corrected α values [31]. Lastly, a series of Spearman's Correlation tests were carried out (SPSS v. 20).

3.2. μ XCT

Since thin-section histological methods are destructive and invasive, we undertook micro-computed tomographic imaging to determine if trauma could be imaged non-invasively. Micro-computed tomographic methods are considered the gold standard for resolving taphonomic alterations to bony structures at a cellular to gross level [32]. Bone blocks were assessed using a Nikon XTH 225 ST micro-focus X-ray computed

tomography (μ XCT) scanner, based at the MIXRAD facility of the South African Nuclear Energy Corporation SOC Ltd (Necsa) [33], prior to and after current application. The scans were volumetrically reconstructed to observe micro-fracture patterns through volume rendered images with Amira (v. 5.4.5). A second set of scans were conducted on five processed and mounted bone thin sections.

4. Results

For each intended charging potential, a range of peak voltages and peak currents resulted (Table 2). Discharges were observed between the bone and the plate in eighty specimens throughout all testing groups (charging potentials of 3.5–8 kV with peak currents of 0–11.5 kA and peak voltages of 3.84–8.3 kV), with accompanying singeing of the bone at the site of the discharge (Fig. 3A). During optimisation, three bone blocks fractured upon application of the impulse. Two blocks were subject to wire-directed impulse application (WDA) at 6 kV. Of these samples the first block experienced a peak voltage (Vp) of 6.24 kV and a peak current (Ip) of 6.72 kA and fractured into two approximately symmetrical parts (Fig. 3B); the second block experienced a Vp of 6.56 kV and a Ip of 8.6 kA, burst into multiple fragments (Fig. 3C). All metal wires were accounted for in both tests where the blocks fractured. With the exclusion of the above-mentioned samples, the remainder of bone blocks did not demonstrate external damage.

Bright field microscopy highlighted patterns of micro-fracturing, while no micro-fracturing was observed in any of the corresponding μ XCT scans (Fig. 4). The average resolution of the μ XCT scans obtained in this study was 21 μ m per voxel, which was therefore simply unable to resolve micro-fractures which had an average diameter of 8.8 μ m (range: 2.33–23.23 μ m) (Fig. 4).

Using light microscopy, short interstitial micro-fractures were observed on all current treated sections as well as control sections originating from only the older female individual (92 years of age at death). This finding is proposed to be due to age related weakening of the mineral matrix of these specimens [34], and thus all interstitial micro-fractures were excluded from analysis.

Qualitative assessment of micro-fractures allowed us to classify histological damage into different classes. This classification was adapted from C.K. Brain's [35] work on burnt bone, where different types were identified based on shape, location, and distribution. In our study we identified micro-fracture classes as: short interstitial, circumferential, circumferential irregular, radiating, and irregular (Figs. 5 and 6).

Data analysis was approached in two iterations. Firstly, individual fracture metrics (fracture area, fracture length, etc.) were analysed independently, followed by analysis of combined fracture data as a ratio of total fracture area and total bone area (TFA/TBA). Intra-class correlations demonstrated a low margin of intra-observer error with agreement scores ranging between 0.861 and 1.000 ($p = 0.001$), throughout all measurements. Inter-observer agreement was low for all measures (ranges: 0.178 to 0.590, $p = 0.001$) except total bone area (TBA), where an agreement score lower boundary of 0.972 and a higher boundary of 1.000 ($p = 0.001$) was identified. This lack of agreement on micro-trauma identification is possibly due to the unfamiliarity of the observers with the histomorphology and the developed classification of microtrauma. This proof-of-concept study thus illustrates that training in histomorphology would be essential for accurate classification of microtrauma. However, a lack of precise classification does not negate the presence and utility of unique lightning-specific lesions.

Fracture types differed between the mode of impulse application ($\chi^2(3) = 13.26$, $p = 0.001$). A greater occurrence of circumferential irregular fractures was identified when current was applied with the parallel plate current (PPA) method ($z = 3.29$, $p = 0.001$) and a lower occurrence of circumferential irregular when using WDA application ($z = -3.29$, $p = 0.001$) (adjusted $\alpha = 0.0063$).

Statistically significant differences were identified as an increase in fracture area at 6 kV compared to 4 kV (Supplementary material: Fig. 1).

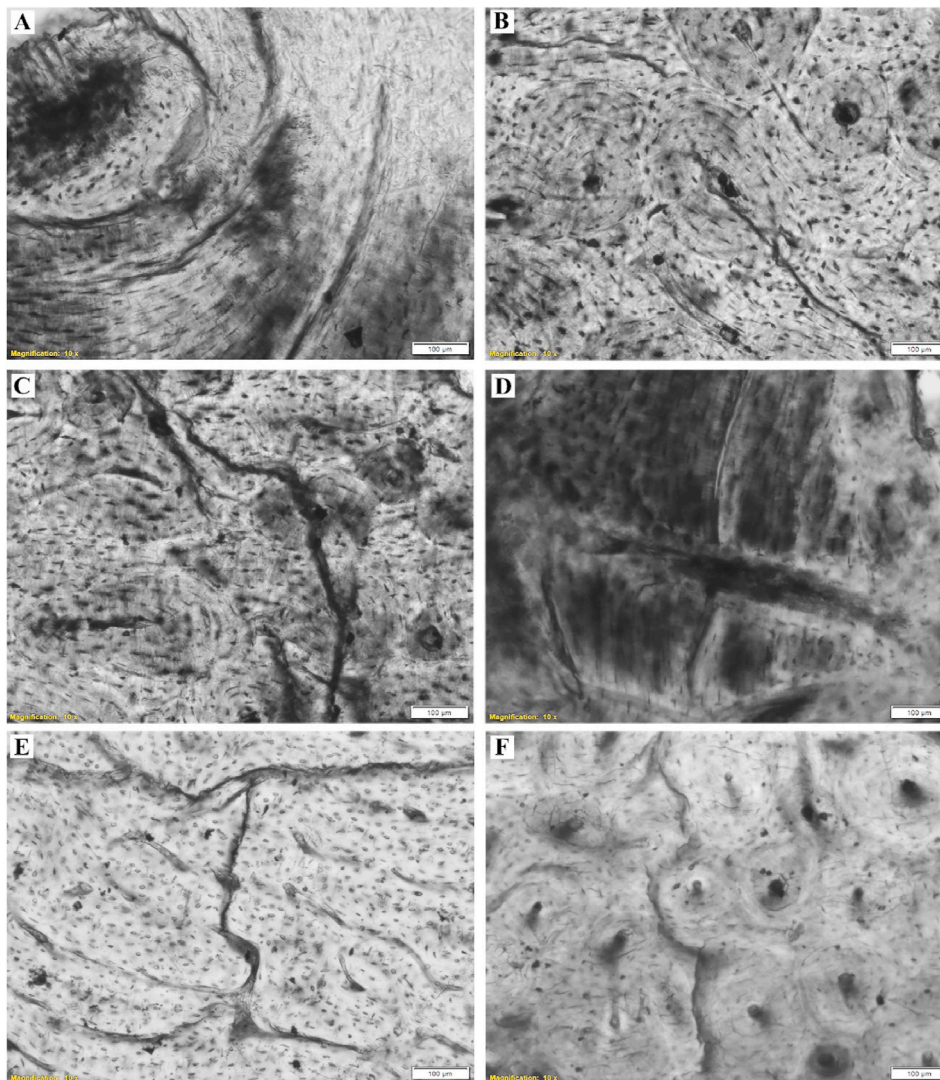


Fig. 7. Comparative actualistic sample micro-trauma examples from previous animal study [20]. Unpublished photomicrographs from the previous study conducted on a giraffe bone (A–D), victim of a lightning strike, and experimentally induced high impulse current micro-trauma to pig bone (E–F). These images demonstrate the varied, yet similar types of damage seen in these samples, with highly irregular damage seen in the giraffe sample (A and C).

These overall differences could be attributed to the wire-directed impulse application increasing from 4 kV through to 6 kV leading to the increase in micro-fracture dimensions. Principal component analysis indicated an association between fracture size variation and irregularity at higher voltages and current intensities (Supplementary material: Tables 1–4, Fig. 2). When further investigating the relationship between micro-trauma and impulse application, a weak positive correlation ($\rho = 0.39$; $p = 0.02$) was identified between fracture number and mean peak current, suggesting a relationship between extent of damage and current intensity. Overall, damage appeared to increase slightly with increasing current intensity regardless of mode of application. The typology of damage appeared to vary with regards to mode of current application. Certain typologies of micro-fracturing were more likely to have larger variation in dimensions than others, as seen with radiating and circumferential micro-fractures (Supplementary material: Fig. 2C). Conversely, a greater presence of irregular and atypical micro-fracture patterns was observed at higher current intensities.

5. Discussion

In death investigation, attribution of lightning strike as cause of death (CoD) falls of the forensic pathologist who uses soft tissue markers

of trauma, such as cutaneous ferning patterns, eardrum rupture, or burns [7,14,36] to aid in attribution of CoD. Typically, autopsy findings are triangulated against witness statements, meteorological services lightning detection data, accident site investigation, and investigation of victim clothing and personal effects. These pathological trauma markers, however, are not necessarily specific to lightning injury mechanics, nor are they always present at autopsy [8]. As such, lightning fatalities can be challenging to identify due to inconsistent expression of trauma [37]. Hence, a holistic approach is required to achieve accurate identification of cause of death in lightning or high voltage related fatalities in a simpler, more easily verifiable manner. To accomplish this goal, actualistic experimentation is often the most effective approach, and this study is the first instance of the application of high impulse current to induce skeletal trauma in human bone tissues.

5.1. Lightning-induced macro-trauma

In this study, current application caused minor thermal disruptions on small, focused areas of the majority of specimens, macroscopically, visible as charring. No other typical signs of thermal disruption, such as heat fractures [21], were seen at a macroscopic level. This could be considered consistent with the nature of impulse currents. Heat

transferred into a sample is measured as heat release rate, which combines both the duration and total heat released, as a better indicator of the total energy entering the sample system [38]. In this case, an impulse current is an excessive energy discharge that may generate a great amount of heat. However, that heat is released over a few microseconds and over a small surface area, which would impede large-scale thermal disruption [22]. We suggest that the mechanism seen in high impulse current trauma to be the generation of a pressure wave around the ionisation channel formed by the traversing high-intensity current, defined as barotrauma [39]. A high-impulse current causes a cylindrical expansion along its path, which results in permanent cavitation of soft gelatine media, temporary cavitation and formation of fissure fractures in harder gelatine media [39]. Similarly, in the current study it is postulated that the impulse current would traverse paths of least resistance through the bone exerting a pressure wave throughout the surrounding matrix causing its fracturing and fragmentation.

Another hypothesis to explain the fracturing visualised in this study could relate to the intrinsic piezoelectric properties of bone [40]. Bone expresses inverse piezoelectric properties, resulting in stress when placed in an electric field [40–42]. The collagen fibres, that dominate the organic matrix of bone, are capable of creating transducing stress on the hydroxyapatite crystals, producing strain that can result in deformation [42]. In the current study, a high impulse current would generate a transient electric field [28], which could impose strong stress on the bone along the current's path, resulting in the deformation of the mineral matrix and possible fracturing.

The electrically induced changes observed in the present study, can be contrasted to thermally induced changes to bone (Table 3). While there is similarity in micro-fracturing patterns, the gross alterations seen in heat treated bone were notably absent from electrically treated samples from the present study (Table 3).

5.2. Lightning-induced micro-trauma

In the present study, resulting micro-trauma was widespread throughout the experimental sample. This was visualised under light microscopy only, with poor resolution of microfractures using μ XCT. While μ XCT has been commonly used as a non-invasive investigation method in geology and bone research [46,47], able to reveal three-dimensional internal features and modification of solid materials, including fracture networks in coal [48,49], beam cone spread and detector area size limit the resolution of scans [50]. We thus propose using nano-focus CT or phase contrast synchrotron scanning to visualise the micro-fractures. Nevertheless, histology and histomorphometry persist as the most efficient and cost-effective method to analyse micro-fracturing patterns caused by high voltage currents in bone.

Consistent with the present study's findings, thermally-induced (burnt) micro-fractures increase in frequency and irregularity as exposure time and heat intensity increase [35,43,45,51]. The micro-trauma observed in the present study is comparable to previously described similar thermally induced micro-trauma patterns. Examples of thermal micro-trauma have been classified as longitudinal fractures, identified both in cortical and trabecular bone [45], or as fissures [44]. Separation of osteon units from surrounding lamellae has also been noted in burnt bone [43], which is morphologically similar to the observed circumferential and circumferential irregular microfractures in this study. Radiating micro-fractures have occasionally been observed in cases of thermal destruction of bone [43]. Imaizumi and colleagues [43] identified "minute cracks" with the osteon canals as the locus of origin in samples treated at temperatures greater than 500 °C, which descriptively correspond with our classification of radiating micro-fractures identified. However, in the present study, these high temperatures (over 500 °C) maintained during thermal degradation, are unlikely given the transient nature of the current applied. The dubious contribution of thermal disruption to the development of the micro-trauma seen in the current study is emphasised by the discrepancy in

presentation of thermal micro-trauma as osteon units have been noted to retain their integrity up to temperatures of 1400 °C [51], which are highly unlikely to have occurred during high impulse current experimentation. As such, these fractures, could be explained parsimoniously by either localised barotrauma [39] or the inversely piezoelectric nature of bone [40–42].

5.3. Micro-trauma in realistic and comparative samples

In an actual lightning flash, multiple current strokes (3–5) tend to traverse the same channel and on average are at much greater intensity (up to 30 kA) [52] than the currents generated for this study, that would inevitably result in cumulative and greater effects than what was demonstrated in this study. The effects of multiple lightning flashes, including the highly irregular and greater extent of micro-trauma was visible in a sample analysed, in a previous study [20]. This sample was obtained from a giraffe struck by an actual lightning strike, and displayed a markedly higher occurrence of micro-fracturing and more irregular micro-fractures overall (Fig. 7A–D). A strong similarity was, however, noted between the giraffe sample micro-trauma patterning and the experimentally induced micro-trauma at higher current intensities in a porcine sample (Fig. 7E and F) in the same study [20]. The microscopic alterations identified in the recovered giraffe bone (Supplementary Material Fig. 3) and in samples from the present study, are inconsistent with other known taphonomic processes, involving fungal or bacterial invasion e.g. [53]. They also appear distinct even from micro-fractures induced by normal weathering, which appear to extend from the surface of the cortical bone and expand towards the medullary cavity as a result of temperature fluctuations below and above freezing [54].

The present study also highlighted the potential importance of bone density on microfracture propagation, as that observed in samples originating from a 92-year-old female. Female individuals over the age of 50 commonly present with decreased bone mineral density [34], which results in bone being more brittle and susceptible to fracturing [55]. Further experimentation among bone material derived from younger and older individuals would be required to confirm the extent of micro-trauma observed.

5.4. Micro-trauma patterns and current pathway

A relative increase in the extent of micro-fracturing and a higher prevalence of irregular fracture types with higher current intensities was also noted in the current study. Increase in irregularity could be attributed to micro-fracture propagation under greater stress imposed by the damaging forces. Both damaging forces and the resultant micro-fracture propagation would be expected to traverse and join, deviating through cement lines and osteon canals [56,57], which are widely considered to experience higher strains [57,58]. The shift in micro-fracture pattern presentation was also seen with circumferential irregular micro-fractures being markedly more common in parallel plate impulse over wire-directed impulse applications, implicating a relationship between current pathway and induced microtrauma.

Identifying exact differences in current path and micro-trauma could lead to an important understanding of high impulse current skeletal trauma and the mechanisms behind it, with the ability to distinguish it from thermal trauma. As such, we suggest that a combination of the piezoelectric nature of bone and localised barotrauma is related to the mechanism of injury. In a real-world setting this mechanism could be corroborated by the suggested path the current would take through a body in a lightning event.

Simulated lightning current pathway through human tissues suggest that 11% of the total current density traverses through the vasculature, despite muscle tissue constituting majority of the model [19]. This is suggestive of a higher affinity for the current to travel through the vasculature [19]. Current travelling through the vasculature, could

potentially enter bone tissue through its vascular supply and course through osteon units (including the Haversian canal) and canalicular network. This pathway would apply a transient electrical field [28] to the bone matrix resulting in inducing stress on the surrounding collagen matrix of the bone [42] leading to micro-fracturing of the bone matrix. Bone exposed to prolonged lower voltage and high-frequency pulsed currents (500 V; 10 kHz; over 66 h) appeared to result in an increase in bone strength and toughness, attributed to a change in collagen fibril arrangement [59]. A stronger impulse current, as was employed in the present study, could similarly result in stronger electric forces acting at high speeds on the collagen fibrils to possibly move them through the mineral matrix, damaging it visibly. Alternatively, as the current traverses the mineral matrix through spaces partly filled with moisture, rapid heating of the confined moisture may result in enough pressure being exerted to induce fracturing [60]. When combined with the transient electric field formed within surrounding tissues (i.e., muscle and connective tissues) and the piezoelectric stress exerted on the bone as a result these mechanisms of injury may explain the micro-trauma observed. The interplay of rapid heating, exerted pressure, and piezoelectric stress are likely the differentiating factors for the traumatic changes seen in high impulse current treated bone compared to bone exposed to prolonged heating, such as burning. A thorough understanding of the mechanisms of injury in bone micro-trauma may aid in determining cause of death in both humans and non-humans, in suspected lightning or high impulse current fatalities.

6. Conclusion

Overall, this study has been the first to look at the effect of high impulse current on human bone. The identified increase in radiating and irregular types of micro-fractures as well as a weak correlation between current and fracture number suggests that the intensity and micro-trauma are positively related. Future studies should employ similar actualistic methodologies to comprehend the contribution of the different interplay of forces in this type of skeletal trauma to resolve a threshold of patterned trauma for distinct lightning fatality identification.

CRediT authorship contribution statement

Nicholas Bacci: Conceptualization, Methodology, Validation, Formal analysis, Investigation, Visualization, Writing – original draft. **Tanya Nadine Augustine:** Supervision, Conceptualization, Methodology, Formal analysis, Investigation, Resources, Visualization, Writing – review & editing. **Hugh G.P. Hunt:** Investigation, Resources, Writing – review & editing. **Ken J. Nixon:** Investigation, Resources, Writing – review & editing. **Jakobus Hoffman:** Investigation, Resources, Data curation, Writing – review & editing. **Lunga Bam:** Investigation, Resources, Data curation, Writing – review & editing. **Frikkie de Beer:** Investigation, Resources, Data curation, Writing – review & editing. **Patrick Randolph-Quinney:** Supervision, Conceptualization, Methodology, Formal analysis, Investigation, Resources, Writing – review & editing.

Declaration of competing interest

The authors declare no competing interests.

Acknowledgments

The authors also express their gratitude to the School of Information and Electrical Engineering, and particularly Harry Lee and Carson McAfee, for their extensive assistance with optimisation of the experimental procedures and set-up of the electrical equipment necessary for this study. Thanks are owed to Martin Bernert, Joshua Davimes, Kyrantia Pather, and Shayla Pillay for their aid.

Appendix A. Supplementary data

Supplementary data to this article can be found online at <https://doi.org/10.1016/j.fsisyn.2021.100206>.

Funding

The authors would like to thank the NRF for funding the equipment at NECSA (grant number: UID 72310) (FDB, JH, LB) as well as funding The Johannesburg Lightning Research Laboratory (Unique Grant number: 98244). They would also like to thank Eskom for the support of the Lightning/EMC Research Group through the TESP programme. Thanks are also due to the Carnegie Corporation Transformation Programme at the University of the Witwatersrand (001.408.8421101) and Wits University URC (001.000.8421101.3113101) for previously funding the Olympus iX51 Inverted Microscope and CellSense Software (TNA) as well as the FRC, University of the Witwatersrand and the JJJ Smieszek grant (NB). The funders had no involvement in study design, collection, analysis, and interpretation of data, or in the writing of the report and submission of the article for publication.

References

- [1] V.A. Rakov, M.A. Uman, *Incidence of lightning*, in: V.A. Rakov, M.A. Uman (Eds.), *Light. Phys. Eff.*, first ed., Cambridge University Press, Cambridge, 2003, pp. 24–54.
- [2] M. Gijben, The lightning climatology of South Africa, *South Afr. J. Sci.* 108 (2012) 1–10.
- [3] M.A. Cooper, R.L. Holle, *Reducing Lightning Injuries Worldwide*, first ed., Springer Natural Hazards, Zug, Switzerland, 2019 <https://doi.org/10.1007/978-3-319-77563-0>.
- [4] C. Gomes, Lightning safety of animals, *Int. J. Biometeorol.* 56 (2012) 1011–1023, <https://doi.org/10.1007/s00484-011-0515-5>.
- [5] T. Gill, *Initial Steps in the Development of a Comprehensive Lightning Climatology of South Africa*, University of the Witwatersrand, Johannesburg, 2009.
- [6] R.L. Holle, The number of documented global lightning fatalities, in: *33rd Int. Conf. Light. Prot. ICLP 2016*, 2016.
- [7] H.G.P. Hunt, R. Blumenthal, K.J. Nixon, C. Gomes, A multidisciplinary forensic analysis of two lightning deaths observed in South Africa, *Int. J. Disaster Risk Reduct.* 51 (2020), 101814, <https://doi.org/10.1016/j.ijdrr.2020.101814>.
- [8] G.C. Hanson, G.R. McIlwraith, Lightning injury: two case histories and a review of management, *Br. Med. J.* 4 (1973) 271–274, <https://doi.org/10.1136/bmj.4.5887.271>.
- [9] K. Wright, H. Davis, R. Wright, S. Diego, The investigation of electrical electrical deaths: a report of 220 fatalities, *J. Forensic Sci.* 25 (1980) 514–521.
- [10] P.F. Mellen, V.W. Weedn, G. Kao, Electrocutation: a review of 155 cases with emphasis on human factors, *J. Forensic Sci.* 37 (1992) 1016–1022. <http://www.ncbi.nlm.nih.gov/pubmed/1506824>.
- [11] T. Bernstein, Effects of electricity and lightning on man and animals, *J. Forensic Sci.* 18 (1973) 3–11. <http://www.ncbi.nlm.nih.gov/pubmed/4781751>.
- [12] M. O'Keefe Gatewood, R.D. Zane, Lightning injuries, *Emerg. Med. Clin.* 22 (2004) 369–403, <https://doi.org/10.1016/j.emc.2004.02.002>.
- [13] C.J. Andrews, A.D. Reinsner, Neurological and neuropsychological consequences of electrical and lightning shock: review and theories of causation, *Neural Regen. Res.* 12 (2017) 677–686, <https://doi.org/10.4103/1673-5374.206636>.
- [14] R. Blumenthal, Lightning fatalities on the South African highveld, *Am. J. Forensic Med. Pathol.* 26 (2005) 66–69, <https://doi.org/10.1097/01.paf.0000154115.12168.46>.
- [15] M. Cherington, S. Olson, P.R. Yarnell, Lightning and lichtenberg figures, *Injury* 34 (2003) 367–371, [https://doi.org/10.1016/S0020-1383\(02\)00313-3](https://doi.org/10.1016/S0020-1383(02)00313-3).
- [16] B.P. Kotak, O. Haddo, M. Iqbal, H. Chissell, Bilateral scapular fractures after electrocution, *J. R. Soc. Med.* 93 (2000) 143–144. <http://www.pubmedcentral.nih.gov/articlerender.fcgi?artid=1297953&tool=pmcentrez&rendertype=abstract>.
- [17] B.D. Lifschultz, E.R. Donoghue, Deaths caused by lightning, *J. Forensic Sci.* 38 (1993) 353–358. <http://www.ncbi.nlm.nih.gov/pubmed/11715217>.
- [18] C. Pfortmueller, Y. Yikun, M. Haberkern, E. Wuest, H. Zimmermann, A. K. Exadaktylos, Injuries, sequelae, and treatment of lightning-induced injuries: 10 years of experience at a swiss trauma center, *Emerg. Med. Int.* 2012 (2012) 1–6, <https://doi.org/10.1155/2012/167698>.
- [19] Y.H. Lee, The Simulated Effect of the Lightning First Short Stroke Current on a Multi-Layered Cylindrical Model of the Human Leg, University of the Witwatersrand, Johannesburg, 2015. <http://hdl.handle.net/10539/22609>.
- [20] N. Bacci, T. Augustine, P. Randolph-Quinney, H. Hunt, K. Nixon, Recognition of lightning-induced trauma to the skeleton: a forensic taphonomic study, in: *ICLP 2014*, 2014, pp. 1299–1302, <https://doi.org/10.1109/ICLP.2014.6973330>.
- [21] P.S. Randolph-Quinney, Burnt human remains I, in: X. Mallett, T. Blythe, R. Berry (Eds.), *Adv. Forensic Hum. Identif.*, first ed., CRC Press, Boca Raton, Florida, 2014, pp. 127–144.

- [22] P.S. Randolph-Quinney, *Burnt human remains II*, in: X. Mallett, T. Blythe, R. Berry (Eds.), *Adv. Forensic Hum. Identif.*, first ed., CRC Press, Boca Raton, Florida, 2014, pp. 145–164.
- [23] S.I. Fairgrieve, *Forensic Cremation: Recovery and Analysis*, first ed., CRC Press, Boca Raton, Florida, 2008 <https://doi.org/10.1111/j.1556-4029.2008.00893.x>.
- [24] D.H. Ubelaker, The forensic evaluation of burned skeletal remains: a synthesis, *Forensic Sci. Int.* 183 (2009) 1–5, <https://doi.org/10.1016/j.forsciint.2008.09.019>.
- [25] D.H. Ubelaker, The forensic evaluation of burned skeletal remains: a synthesis, *Forensic Sci. Int.* 183 (2009) 1–5, <https://doi.org/10.1016/j.forsciint.2008.09.019>.
- [26] M.L. Hillier, L.S. Bell, Differentiating human bone from animal bone: a review of histological methods, *J. Forensic Sci.* 52 (2007) 249–263, <https://doi.org/10.1111/j.1556-4029.2006.00368.x>.
- [27] D. Kind, *An Introduction to High-Voltage Experimental Technique*, first ed., Vieweg & Teubner Verlag, Wiesbaden, 1978 <https://doi.org/10.1007/978-3-322-91763-8>.
- [28] K. Schon, *High Impulse Voltage and Current Measurement Techniques*, first ed., 2013, <https://doi.org/10.1007/978-3-319-00378-8>. Springer, Switzerland.
- [29] W. Hauschild, E. Lemke, *High-voltage Test and Measuring Techniques*, 2019, <https://doi.org/10.1007/978-3-319-97460-6>.
- [30] G.J.R. Maat, R.P.M. Van Den Bos, M. Aarents, Manual preparation of ground sections for the microscopy of natural bone tissue: update and modification of Frost's rapid manual method, *Int. J. Osteoarchaeol.* 11 (2001) 366–374, <https://doi.org/10.1002/oa.578>.
- [31] T.M. Beasley, R.E. Schumacher, Multiple regression approach to analyzing contingency tables: post hoc and planned comparison procedures, *J. Exp. Educ.* 64 (1995) 79–93, <https://doi.org/10.1080/00220973.1995.9943797>.
- [32] P.S. Randolph-Quinney, S.D. Haines, A. Kruger, The use of three-dimensional scanning and surface capture methods in recording forensic taphonomic traces: issues of technology, visualisation, and validation, in: P.M. Barone, W.J.M. Goren (Eds.), *Multidiscip. Approaches to Forensic Archaeol.*, first ed., Springer, Berlin, 2018, pp. 115–130.
- [33] J. Hoffman, F. De Beer, Characteristics of the micro-focus x-ray tomography facility (MIXRAD) at Necsa in South Africa, in: 18th World Conf. Nondestruct. Test., Durban, South Africa, 2012, pp. 1–12. http://www.ndt.net/article/wcndt2012/papers/37_wcndtfinal00037.pdf.
- [34] N.E. Lane, Epidemiology, etiology, and diagnosis of osteoporosis, *Am. J. Obstet. Gynecol.* 194 (2006) 3–11, <https://doi.org/10.1016/j.ajog.2005.08.047>.
- [35] C.K. Brain, The occurrence of burnt bones at swartkrans and their implications for the control of fire by early hominids, in: C.K. Brain, A. Sillen, T. Hoering (Eds.), *Swart. A Cave's Chron. Early Man*, first ed., The Transvaal Museum, Pretoria, South Africa, 1991, pp. 229–235. https://hdl.handle.net/10520/AJA090799001_71.
- [36] H.G.P. Hunt, Lightning location system detections as evidence: a unique bayesian framework, *IEEE Trans. Geosci. Rem. Sens.* (2020) 1–11, <https://doi.org/10.1109/tgrs.2020.3000680>.
- [37] I.R. Jandrell, R. Blumenthal, R.B. Anderson, E. Trengove, Recent lightning research in South Africa with a special focus on keraunopathology, in: 16th Int. Symp. High Volt. Eng., Cape town, South Africa, 2009, pp. 24–28.
- [38] M.L. Janssens, Material flammability, in: *Handb. Environ. Degrad. Mater.*, Elsevier, 2012, pp. 283–307, <https://doi.org/10.1016/B978-1-4377-3455-3.00009-2>.
- [39] R. Blumenthal, I.R. Jandrell, N.J. West, Does a sixth mechanism exist to explain lightning injuries? *Am. J. Forensic Med. Pathol.* 33 (2012) 222–226, <https://doi.org/10.1097/PAF.0b013e31822d319b>.
- [40] E. Fukada, I. Yasuda, On the piezoelectric effect of bone, *J. Phys. Soc. Japan.* 12 (1957) 1158–1162, <https://doi.org/10.1143/JPSJ.12.1158>.
- [41] C.A.L. Bassett, R.O. Becker, Generation of electric potentials by bone in response to mechanical stress, *Science* 137 (1962) 1063–1064, <https://doi.org/10.1126/science.137.3535.1063> (80-).
- [42] D.C.F. Wieland, C. Krywka, E. Mick, R. Willumeit-römer, R. Bader, D. Kluess, Investigation of the inverse piezoelectric effect of trabecular bone on a micrometer length scale using synchrotron radiation, *Acta Biomater.* 25 (2015) 339–346, <https://doi.org/10.1016/j.actbio.2015.07.021>.
- [43] K. Imaizumi, K. Taniguchi, Y. Ogawa, DNA survival and physical and histological properties of heat-induced alterations in burnt bones, *Int. J. Leg. Med.* 128 (2014) 439–446, <https://doi.org/10.1007/s00414-014-0988-y>.
- [44] G. Quatrehomme, M. Bolla, M. Muller, J.P. Rocca, G. Grévin, P. Baillet, A. Ollier, Experimental single controlled study of burned bones: contribution of scanning electron microscopy, *J. Forensic Sci.* 43 (1998) 417–422. <http://www.ncbi.nlm.nih.gov/pubmed/9544556>.
- [45] R. Fernández Castillo, D.H. Ubelaker, J.A.L. Acosta, R.J.E. de la Rosa, I.G. Garcia, Effect of temperature on bone tissue: histological changes, *J. Forensic Sci.* 58 (2013) 578–582, <https://doi.org/10.1111/1556-4029.12093>.
- [46] M.L. Bouxsein, S.K. Boyd, B.A. Christiansen, R.E. Guldberg, K.J. Jepsen, R. Müller, Guidelines for assessment of bone microstructure in rodents using micro-computed tomography, *J. Bone Miner. Res.* 25 (2010) 1468–1486, <https://doi.org/10.1002/jbmr.141>.
- [47] A. Golab, C.R. Ward, A. Permana, P. Lennox, P. Botha, High-resolution three-dimensional imaging of coal using microfocus X-ray computed tomography, with special reference to modes of mineral occurrence, *Int. J. Coal Geol.* 113 (2013) 97–108, <https://doi.org/10.1016/j.coal.2012.04.011>.
- [48] X. Shi, J. Pan, Q. Hou, Y. Jin, Z. Wang, Q. Niu, M. Li, Micrometer-scale fractures in coal related to coal rank based on micro-CT scanning and fractal theory, *Fuel* 212 (2018) 162–172, <https://doi.org/10.1016/j.fuel.2017.09.115>.
- [49] J. Viljoen, Q.P. Campbell, M. Le Roux, J. Hoffman, The qualification of coal degradation with the aid of micro-focus computed tomography, *South Afr. J. Sci.* 111 (2015) 1–10, <https://doi.org/10.17159/sajs.2015/20140025>.
- [50] T. Buzug, *Computed Tomography: from Photon Statistics to Modern Cone-Beam CT*, first ed., Springer, Leipzig, Germany, 2008 <https://doi.org/10.1007/978-3-540-39408-2>.
- [51] J.L. Holden, P.P. Phakey, J.G. Clement, Scanning electron microscope observations of heat-treated human bone, *Forensic Sci. Int.* 74 (1995) 29–45, [https://doi.org/10.1016/0379-0738\(95\)01735-2](https://doi.org/10.1016/0379-0738(95)01735-2).
- [52] M.A. Uman, *Physics and effects*, in: V.A. Rakov, M.A. Uman (Eds.), *Light. Physics Eff.*, first ed., Cambridge University Press, Cambridge, 2003, pp. 1–12.
- [53] I. Kontopoulou, P. Nystrom, L. White, Experimental taphonomy: post-mortem microstructural modifications in *Sus scrofa* domesticus bone, *Forensic Sci. Int.* 266 (2016) 320–328, <https://doi.org/10.1016/j.forsciint.2016.06.024>.
- [54] J.T. Pokines, R.E. King, D.D. Graham, A.K. Costello, D.M. Adams, J.M. Pendray, K. Rao, D. Siwek, The effects of experimental freeze-thaw cycles to bone as a component of subaerial weathering, *J. Archaeol. Sci. Rep.* 6 (2016) 594–602, <https://doi.org/10.1016/j.jasrep.2016.03.023>.
- [55] M.A. Clynes, N.C. Harvey, E.M. Curtis, N.R. Fuggle, E.M. Dennison, C. Cooper, The epidemiology of osteoporosis, *Br. Med. Bull.* (2020) 1–13, <https://doi.org/10.1093/bmb/ldaa005>, 00.
- [56] R.K. Nalla, J.S. Stölken, J.H. Kinney, R.O. Ritchie, Fracture in human cortical bone: local fracture criteria and toughening mechanisms, *J. Biomech.* 38 (2005) 1517–1525, <https://doi.org/10.1016/j.jbiomech.2004.07.010>.
- [57] F. Libonati, L. Vergani, Bone toughness and crack propagation: an experimental study, *Procedia Eng.* 74 (2014) 464–467, <https://doi.org/10.1016/j.proeng.2014.06.298>.
- [58] D.P. Nicoletta, A.E. Nicholls, J. Lankford, D.T. Davy, Machine vision photogrammetry: a technique for measurement of microstructural strain in cortical bone, *J. Biomech.* 34 (2001) 135–139, [https://doi.org/10.1016/S0021-9290\(00\)00163-9](https://doi.org/10.1016/S0021-9290(00)00163-9).
- [59] H. Asgarifar, A. Oloyede, F. Zare, The effect of high voltage, high frequency pulsed electric field on slain ovine cortical bone, *J. Med. Signals Sens.* 4 (2014) 113–121.
- [60] C.Y. Hui, V. Muralidharan, M.O. Thompson, Steam pressure induced in crack-like cavities in moisture saturated polymer matrix composites during rapid heating, *Int. J. Solid Struct.* 42 (2005) 1055–1072, <https://doi.org/10.1016/j.ijsolstr.2004.06.058>.